Correlation in the transition-metal-based Heusler compounds Co_2MnSi and Co_2FeSi

Hem Chandra Kandpal, Gerhard H. Fecher, and Claudia Felser*
Institut für Anorganische und Analytische Chemie, Johannes Gutenberg Universität, D-55099 Mainz, Germany

Gerd Schönhense
Institut für Physik, Johannes Gutenberg Universität, D-55099 Mainz, Germany
(Received 22 November 2005; published 20 March 2006)

Half-metallic ferromagnets, such as the Heusler compounds with formula X_2YZ, are expected to show an integer value for the spin magnetic moment. In contrast to experiments, calculations give noninteger values in certain cases where the compounds are based on X=Co. In order to explain deviations of the magnetic moment calculated for such compounds, the dependence of the electronic structure on the lattice parameter was studied theoretically. In the local density approximation (LDA), the minimum total energy of Co_2FeSi is found for the experimental lattice parameter, but the calculated magnetic moment is approximately 12% too low. In addition, half-metallic ferromagnetism and a magnetic moment equal to the experimental value of $6\mu_B$ are found only after increasing the lattice parameter by more than 6%. To overcome these discrepancies, the LDA+U scheme was used to respect on-site electron correlation in the calculations. For Co_2FeSi, these calculations showed that an effective Coulomb exchange interaction $U_{eff}=U-J$ in the range of approximately 2–5 eV leads to half-metallic ferromagnetism and to the measured integer magnetic moment at the measured lattice parameter. Finally, it is shown for Co_2MnSi that correlation may also serve to destroy the half-metallic behavior if the correlation becomes too strong (above 2 eV for Co_2MnSi and above 5 eV for Co_2FeSi). These findings indicate that on-site correlation may play an important role in the description of Heusler compounds with localized moments.

DOI: 10.1103/PhysRevB.73.094422 PACS number(s): 75.30.Cr, 71.20.Lp, 75.50.Cc

I. INTRODUCTION

de Groot *et al.*[1] first predicted half-metallic ferromagnetism for the Heusler-like compound NiMnSb. A half-metallic ferromagnet is a material with a gap in one of the spin states at the Fermi energy (ϵ_F)—for example, such that the majority states are conducting and the minority states are semiconducting. Half-metallic ferromagnets (HMFs) are expected to exhibit a real gap in the minority (or majority) density of states (DOS). In compounds with integer site occupancies, this gap requires the magnetic moment to be an integer because the number of occupied minority states is integer. It should be noted that the HMF character is lost if even a small deviation from an integer value is observed.

Certain X_2YZ Heusler compounds have also been predicted to show half-metallic ferromagnetism.[2] Heusler compounds containing Co and Mn have attracted particular attention as they are strongly ferromagnetic with high Curie temperatures (above 900 K).[3] One of these compounds—Co_2MnSi—is an attractive candidate for many applications in spin dependent electronics. This compound was used by several groups to produce thin films[4–9] and devices.[10,11] It was recently shown that Co_2FeSi is also a very good candidate since it exhibits a very high Curie temperature of 1100 K and a magnetic moment of $6\mu_B$.[12] This compound is somewhat peculiar in regards to its Curie temperature and magnetic moment because both values are the highest observed until now in this class of materials.

In Heusler as well as other compounds, the half-metallic ferromagnetism has not yet been unambiguously confirmed by experiments, although there is strong evidence in some cases. Despite a large amount of work on Heusler compounds that contain Co and Mn,[5,13–22] a breakthrough is still required to prove the existence of half-metallic ferromagnetism in these materials.

The electronic structure plays an important role in determining the magnetic properties of Heusler compounds. In this work, a comprehensive investigation of the equilibrium structural, electronic, and magnetic properties of Co_2FeSi is presented and compared to the properties of Co_2MnSi. The dependence of the magnetic moment on the lattice parameter was analyzed, focusing on the differences between the local spin density approximation and the generalized gradient approximation (GGA) treatments. A series of calculations for Heusler compounds based on Co_2 was performed and showed that almost all Heusler compounds based on Co_2 exhibit half-metallic ferromagnetism,[23] results that are in agreement with Ref. 24. The Slater-Pauling rule[12,24–27] applies to most Heusler compounds based on Co_2 and may be used to estimate their magnetic moments. According to this rule, the magnetic moment of Co_2FeSi is expected to be $6\mu_B$ per unit cell.

The impetus for this work was a recent experimental study that was devoted to measuring the magnetic moment and Curie temperature of the Co_2FeSi compound.[12] To provide a concise picture of the Co_2YSi systems (Y=Mn, Fe), a theoretical investigation will be presented utilizing the local (spin) density approximation [L(S)DA], the GGA, and the LDA+U methods.

II. COMPUTATIONAL DETAILS

Heusler compounds[28] belong to a group of ternary intermetallics with the stoichiometric composition X_2YZ ordered

in an $L2_1$-type structure, space group $Fm\bar{3}m$, and many of these compounds are ferromagnetic.[29] Remarkably, the prototype Cu_2MnAl is a ferromagnet even though none of its constituents is ferromagnetic.[30] In general, the X and Y atoms are transition metals and Z is a main group element. In some cases, Y is replaced by a rare-earth element. The X atoms are placed on 8a (1/4,1/4,1/4) Wyckoff positions and the Y and Z atoms on 4a (0,0,0) and 4b (1/2,1/2,1/2) positions, respectively. The cubic $L2_1$ structure consists of four interpenetrating fcc lattices, two of which are equally occupied by X. The latter twoX_2 fcc sublattices combine to form a simple cubic sublattice. The compound may thus be viewed as being a CsCl ($B2$) superstructure with the cubic vacancies of the X_2 sublattice alternatingly filled by Y or Z atoms. Other than in a simple CsCl structure, the nearest-neighbor polyhedra of each X atom are given by two different tetrahedra (rotated by 90° with respect to each other) that are built from either Y or Z atoms. The Γ point of the paramagnetic structure has the symmetry O_h. However, the wave functions at the Γ point have to be described by C_{4h} in the ferromagnetic state (magnetization along [001]) to account for the correct transformation of the electron spin.

Self-consistent band-structure calculations were carried out using the full-potential linear augmented-plane-wave (FLAPW) method as provided by Blaha *et al.* (WIEN2k).[31] The calculations were performed using the von Barth-Hedin[32] parametrization of the exchange-correlation functional within the LSDA. In addition, the Perdew-Burke-Ernzerhof[33] implementation of the GGA was used. The GGA specifically accounts for density gradients that are neglected in the pure L(S)DA. The energy threshold between the core and valence states was set to −6 Ry. Here $2.3a_{Bohr}$ were considered for the muffin-tin radii (R_{MT}) of all the atoms, and this resulted in nearly touching spheres, and 455 irreducible k points of a $25\times25\times25$ mesh were used for Brillouin zone integration. The number of plane waves was restricted to $R_{MT}\times k_{max}=7$. The energy convergence criterion was set to 10^{-5}. The charge convergence was monitored simultaneously, and the calculation was restarted if it was still greater than 10^{-3}.

Finally, the LDA+U method[34] was used to account for on-site correlation at the transition-metal sites. The LDA+U method accounts for an orbital dependence of the Coulomb and exchange interaction that is absent in the pure LDA. The effective Coulomb exchange interaction ($U_{eff}=U-J$) was used here for the calculations. This particular scheme is used in WIEN2k to include double-counting corrections. The framework of density functional theory (DFT) is left when the LDA+U method is applied. However, it is one of the most popular and easiest approaches used for considering electron-electron correlation. When applied to Co_2FeSi, it will be shown that the LDA+U method gives qualitative and quantitative improvements over the plain LDA or GGA approaches.

III. RESULTS AND DISCUSSION

The main focus was on the magnetic moment as this shows a very strong discrepancy when the experimental and calculated values reported for Co_2FeSi are compared. Niculescu *et al.*[35] have already reported a magnetic moment of $5.9\mu_B$ per unit cell at 10 K, whereas band-structure calculations using the screened Korringa-Kohn-Rostocker (KKR) method later predicted a magnetic moment of only $5.27\mu_B$.[24] The present LSDA calculations (FLAPW) also produced a total magnetic moment of only $5.29\mu_B$. This value is much lower than the measured value of approximately $6\mu_B$.[12] Such a large discrepancy clearly indicates that the actual electronic structure of this compound is different from the calculated structure. Although the calculations for Co_2MnSi agree with the experiment in regards to the magnetic moment, their reliability concerning the details of the electronic structure may have to be called into question as long as the differences obtained for Co_2FeSi remain unexplained.

The discrepancy between experiment and calculation was not removed when the GGA parametrization was used, resulting in a value that was still too low ($5.56\mu_B$). Inspecting the spin-resolved DOS and band structure revealed the appearance of a gap in the minority bands, but located below the Fermi energy [see Figs. 8(b) and 9(e) in Sec. III B 2]. This is one reason why the magnetic moment is too low and not an integer. In the following, details of the electronic structure calculations will be discussed.

A. Structure optimization

A structural optimization was first performed for Co_2FeSi and Co_2MnSi to determine if the experimental lattice parameter minimizes the total energy. It was found that the optimized lattice parameter from the calculation agrees very well with the experimental values of $a_{expt,Fe}=5.64$ Å and $a_{expt,Mn}=5.645$ Å. Within the FLAPW scheme, the structure optimization for Co_2YSi (Y=Mn,Fe)was performed using the GGA parametrization and a spin-polarized (ferromagnetic) setup. The initial crystal structural parameter for $\Delta a/a=0$ is taken from the experimental value a_{expt} and varied in steps of 2%. For each of the different a parameters, the iteration procedure was performed up to self-consistency. The energy minimum then defines the optimal value of a.

For Co_2FeSi, the energy minimum (ferromagnetic) was found to appear at $a=5.63$ Å (corresponding to $\Delta a/a_{expt}\approx-0.2\%$; see Fig. 1, GGA). It was also found that the ferromagnetic (spin-polarized) configuration has a lower minimum total energy than that found in the paramagnetic (non-spin-polarized) case, which is not shown here. Similar calculations for Co_2MnSi showed that the energy minimum appears at $a=5.651$ Å (corresponding to $\Delta a/a_{expt}\approx+0.1\%$).

In addition, Fig. 1 displays the results of a structural optimization using the LDA+U scheme with U_{eff} as a variational parameter. The results of this optimization, which were performed for different values of U_{eff}, will be discussed below in Sec. III B.

Electronic structure and lattice parameter

To understand why the LSDA and GGA do not produce the expected magnetic moment and position of the gap, the dependence of both observables on the lattice parameter was carefully examined for Co_2FeSi as well as Co_2MnSi. It is

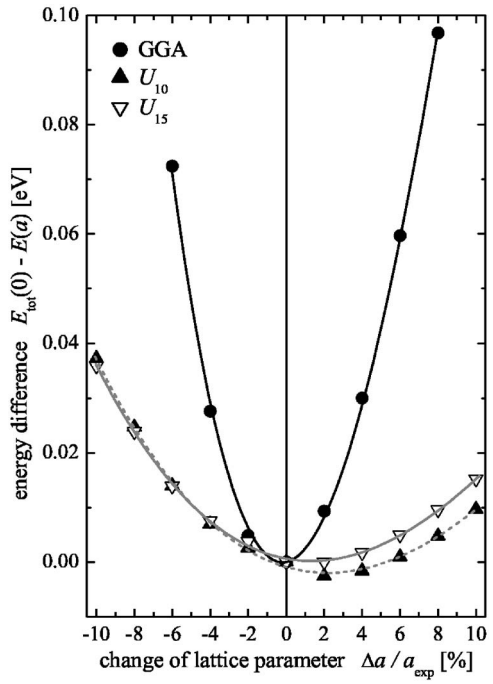

FIG. 1. Structural optimization for Co_2FeSi. The change of the total energy as a function of the lattice parameter (a_0=5.64 Å) is shown. The GGA results are compared to the LDA+U calculations with different U_{eff} (see text). Note that all energy scales are shifted to $E_{tot}(0)=0$ for better comparison. The lines are results from a polynomial fit.

important to compare the electronic structure of Co_2FeSi with Co_2MnSi as the latter is predicted to be a half-metallic ferromagnet with a measured magnetic moment of $5\mu_B$, which is found in calculations that use the experimental lattice parameter. However, a spin polarization of only about 55%, as determined by point contact Andreev reflection spectroscopy,[36,37] was obtained for this compound. The spin polarization at the Fermi energy determined by means of photoemission was even lower (8%–11%).[8]

The calculated total and site-specific magnetic moments are shown in Fig. 2 for Co_2FeSi and Co_2MnSi. In Co_2FeSi [Fig. 2(b)], the calculated atomic-resolved magnetic moments of both Co and Fe increase with a, and the overall magnetic moment follows the same trend, increasing from $4.96\mu_B$ to more than $6\mu_B$ as a increases. The experimental value of $6\mu_B$ is found when the lattice parameter is increased by approximately 6%–10%. When the lattice parameter changes by more than +6%, the site-specific moments appear to saturate at about $1.5\mu_B$ and $3\mu_B$ for Co and Fe, respectively. (Slightly higher values are compensated by an antiparallel alignment of the moments at the Si sites and in the interstitial space between the muffin-tin spheres.)

The total magnetic moment of Co_2MnSi [Fig. 2(a)] also increases slightly with the lattice parameter, but it stays at $5\mu_B$ when a changes in the range of ±6%. There is a significant change in the magnetic moment at Mn sites; it increases as the lattice parameter increases. At the same time, the magnetic moment of Co decreases. Thus the Co moment counterbalances the Mn moment such that the overall magnetic moment remains constant as the lattice parameter changes.

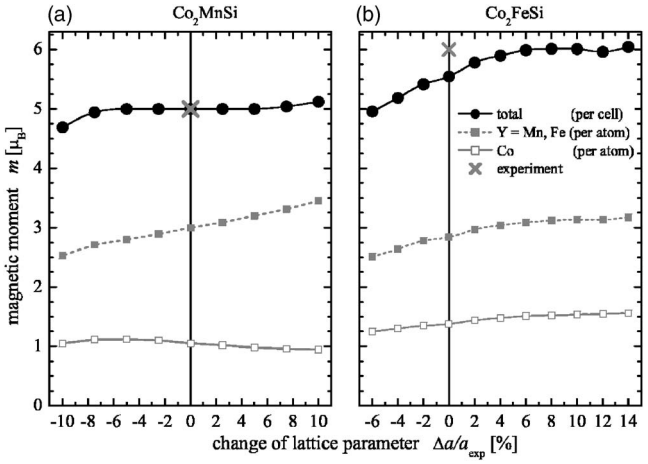

FIG. 2. Lattice parameter dependence of the magnetic moments. The total and site-specific magnetic moments of Co_2MnSi (a) and Co_2FeSi (b) as functions of the lattice parameter are shown. Experimental values are indicated by a cross. The experimental lattice parameters are $a_{Y=Mn}$=5.645 Å and $a_{Y=Fe}$=5.64 Å. Lines are drawn through the calculated values for clarity.

At this point, it can be said that a moderate change of the lattice parameter does not change the overall magnetic moment of Co_2MnSi. The case of Co_2FeSi is completely different: an overall change of about $1\mu_B$ is observed in the same range of $\Delta a/a$ as for Co_2MnSi. Overall, the magnetic moment of Co_2FeSi is less stable against variations of the lattice parameter (at least if using the same parameters for integration and convergence criteria as for the Co_2MnSi calculations). It exhibits some fluctuations about the integer value at very large values of the lattice parameter.

As was explained in detail by Kübler *et al.*,[27,38] the formation of the gap and the localized magnetic moments in Heusler compounds is due to hybridization. There is a close relationship between the magnetic moment and the HMF character. The appearance of the gap in the minority density constrains the number of minority electrons to be integer.[58] However, an integer value of the magnetic moment may not automatically result in a real gap in the minority (or majority) density. The band structure of Co_2FeSi (see also below in Sec. III B 2) already displayed a small gap in the minority states in the calculation for the experimental lattice parameter, but this gap is located below the Fermi energy (ϵ_F). Therefore, the band structure was examined more closely to check if the integer moment is related to the appearance of a real HMF minority gap.

Figure 3 shows the dependence of the extremal energies of the lower (valence) band and upper (conduction) band of the minority states enveloping the gap. For both materials, the magnetic moment must be an integer in the region where ϵ_F falls into the gap (gray shaded areas in Fig. 3), which is the region of half-metallic ferromagnetism.

Figure 3(a) shows the dependence of the gap on the lattice parameter for Co_2MnSi. The shaded area corresponds to the region of half-metallic ferromagnetism. It is clearly seen that Co_2MnSi behaves like a HMF within a ±5% change of the lattice parameter. Therefore, a moderate change of the lattice parameter does not change the HMF behavior of Co_2MnSi.

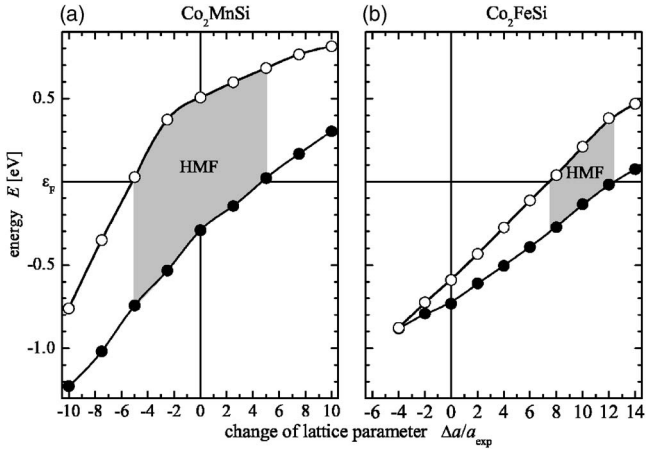

FIG. 3. Dependence of the minority band gap on the lattice parameter. The extremal energies of the gap involving states for Co_2MnSi (a) and Co_2FeSi (b) are shown. The shaded areas indicate the region of half-metallic ferromagnetism. Lines are drawn for clarity.

Figure 3(b) shows the dependence of the gap on the lattice parameter for Co_2FeSi. It is seen that the gap encloses the Fermi energy for a $7.5\%-12\%$ increase in the lattice parameter. The gap is completely closed for lattice parameters that are 4% less than a_{expt}. The gap ($\Delta E_{max}=0.4$ eV at +12%) is obviously smaller than that for Co_2MnSi ($\Delta E_{max}=0.9$ eV at -2.5%), and appears in a narrower range of the lattice parameter. It can be seen that the HMF character and thus the integer magnetic moment are more stable against a variation of the lattice parameter in Co_2MnSi than in Co_2FeSi.

An increase in the lattice parameter by $8\%-12\%$ is needed to explain the magnetic moment of Co_2FeSi, corresponds to a volume expansion of about $26\%-40\%$. Such a large expansion of the crystal volume by about 1/3 is rather unrealistic and is far greater than the expected uncertainties in the experimental determination of a. However, it may be interesting to check what changes in the electronic structure are caused by such an expansion.

The DOS and the band structure of Co_2FeSi are shown in Fig. 4 for the increased lattice parameter. The calculations were performed using the GGA scheme. An expansion of $\Delta a/a=10\%$ was used in the calculation (for $\Delta a/a=0$ see Sec. III B 2 and also Ref. 12). This particular value was chosen because it is the value at which the Fermi energy lies just in the middle of the gap of the minority DOS [see Figs. 4(a) and 4(b)], securely placing the material in an HMF state.

There are no minority states at ϵ_F, confirming that the compound is in an HMF state. The high density below ϵ_F is dominated by d states located at Co and Fe sites. The small density of states near ϵ_F in the majority DOS emerges from the strongly dispersing majority bands crossing the Fermi energy. From the spin-resolved bands, it is seen that the majority bands cross or touch the Fermi energy (ϵ_F) in rather all directions of high symmetry. On the other hand, the minority bands exhibit a clear gap around ϵ_F. For Co_2FeSi, the width of the gap is given by the energies of the highest occupied band at the Γ point and the lowest unoccupied band at the Γ or X point. The smaller value is found between Γ and X; thus, it is an indirect gap. The conclusion drawn from the

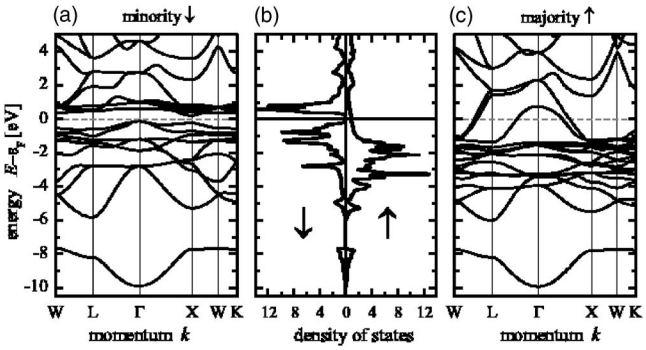

FIG. 4. Electronic structure of Co_2FeSi with increased lattice parameter (LSDA-GGA, $a=6.2$ Å).

displayed electronic structure is that the states around the Fermi energy are strongly spin polarized and that, according to the calculations, the system is indeed a half-metallic ferromagnet, at least for an increased lattice parameter. The gap in the minority DOS has the compelling result that the magnetic moment is integer with a value of $6\mu_B$, a result that is expected from experiment.

The change of the electronic structure with the lattice parameter is clear for two reasons. The first is that a change of the band gradients is expected from a free-electron-like band structure, as well as a mere shift of ϵ_F due to the accompanying changes in the DOS. The second is that a difference in both overlap and hopping integrals is expected from a tight-binding-like approach. In particular, they will be smaller for larger values of the lattice parameter. With a decrease in a, the interaction between the atoms becomes stronger and the higher overlap results in a stronger delocalization of the electrons. The overlap is obviously too large in the calculation that uses the experimental lattice parameter of Co_2FeSi. On the other hand, for nearly HMF compounds, if the LSDA (GGA) calculations result in the correct electronic structure, the fact that small deviations of the magnetic moment from integer values can be compensated by small variations of the lattice parameter can be used. Unfortunately, the opposite is also true. If the calculated Fermi energy is not just in the middle of the minority gap, then a small deviation of the lattice parameter may destroy the HMF character.

The major conclusion that can be drawn from the needed increase of the lattice parameter of Co_2FeSi is that the plain LSDA (GGA) calculations are not sufficient to simultaneously explain both its electronic and geometric structure, and thus may also fail for similar compounds. Moreover, it is suggested that electron-electron correlation might play an important role in opening the gap in the minority states and for obtaining a magnetic moment with an integer value. For both the lattice parameter and the magnetic moment, the experimental results must be verified independently of the material. In the following section, an analysis will be performed to examine if this goal can possibly be reached by inclusion of correlation.

B. Electron correlation

The relative importance of itinerant versus localized properties of d electrons in metal alloys has already been dis-

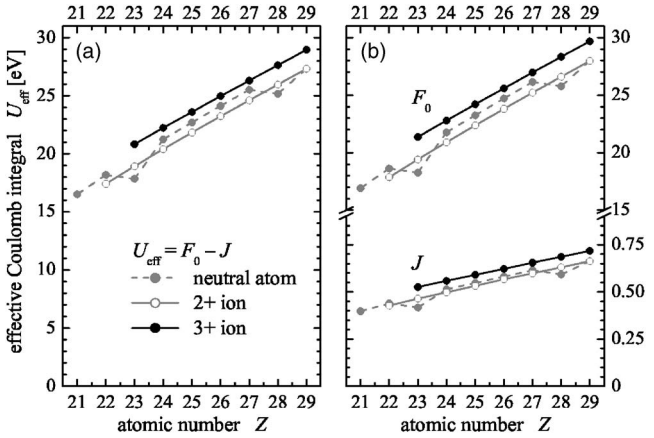

FIG. 5. Atomic Coulomb exchange parameter. The values were calculated for the 3*d* transition metals using the neutral as well as the most common ionic configurations. Note that the values for *J* in (b) are shown on an expanded scale below the break.

cussed by van Vleck[39] and Slater.[25,40] As was first mentioned by Pauling for Cu_2MnAl,[26] Heusler compounds are generally thought of as systems that exhibit localized magnetic moments. In particular, the magnetic moments of the Co_2YZ half-metallic ferromagnets strictly follow the *localized* part of the well-known Slater-Pauling curve.[12] It is clear that the *d* electrons are delocalized in metals. Thus, the question about correlation in transition-metal-based compounds is as follows: to what extent is the on-site Coulomb interaction between *d* electrons preserved so that important atomic properties like Hund's rule are significant and magnetic properties are at least partially determined? [41]

After structural optimization failed to explain the magnetic moment of Co_2FeSi, it was thought that inclusion of electron-electron correlation may be necessary in order to respect a partial *localization* of the *d* electrons in a better way. For this reason, the LDA+*U* method was used to recalculate the electronic structure of Co_2MnSi and Co_2FeSi.

The LDA+*U* scheme is designed to model localized states when on-site Coulomb interactions become important. It provides a self-energy correction to localized states that are embedded in delocalized states. The energy *U* of the Coulomb interaction is rather large in free atoms (17–27 eV in 3*d* transition metals; see Fig. 5), while screening in solids results in much smaller values[42] (for example, 4.5 eV in bcc Fe). In the present work, the value of the effective Coulomb exchange interaction $U_{eff}=U-J$ was varied in order to reproduce the measured magnetic moment. A magnetic moment of $6\mu_B$ resulted for a U_{eff} of 2.5–5.0 eV for Co and, simultaneously, for a U_{eff} of 2.4–4.8 eV for Fe. As calculated from the corresponding Slater integrals by using Cowan's program,[43] these values for U_{eff} correspond to about 7%–20% of the free-atom values.

The average on-site Coulomb energy of pairs (ij) of equivalent electrons $(i=j)$ is calculated from the Slater integrals F_k to be

$$E_{ii} = F_{0,ii} - \frac{2l_i+1}{4l_i+1} \sum \begin{pmatrix} l_i & k & l_i \\ 0 & 0 & 0 \end{pmatrix}^2 F_{k,ii}. \quad (1)$$

The sum runs over all $k>0$ resulting in nonzero $3j$ symbols. The $3j$ symbols vanish for odd *k*, and $k_{max}=2l_i=4$ for *d* electrons so that Eq. (1) becomes

$$E_{dd} = F_0 - \frac{2}{63}F_2 - \frac{2}{63}F_4, \quad (2)$$

where the on-site Coulomb integral is $U=F_0$ and all integrals are calculated for $l=2$. The exchange integral is given by

$$J = \frac{2}{63}(F_2 + F_4). \quad (3)$$

Equation (3), as calculated from Cowans's work,[43] differs from the equation reported by Anisimov *et al.*,[34] giving a factor of 1/14 instead of 2/63, for unknown reasons.[59]

The atomic values of $U=F_0$, *J*, and $U_{eff}=E_{dd}$, as calculated for the 3*d* transition metals, are displayed in Fig. 5. In the following, we will denote the U_{eff} values by U_x, where the subscript *x* stands for the values (in %) relative to the atomic values (neutral atoms). It should be mentioned that the effect of screening in solids will mainly influence *U* rather than the exchange integrals *J*. On the other hand, the values of *J* also depend on the ionicity [see Fig. 5(b)], which will be different in solids and which will depend upon the compound under investigation. From a practical point of view, the use of U_x relative to the atomic values allows comparisons to be made between different systems that are easier to accomplish than those that use separate values for all quantities and atoms.

A structural optimization was first performed for Co_2FeSi using different values of U_{eff} in the calculations (see also Sec. III A). It can be seen from Fig. 1 that adding U_{eff} results in a less pronounced change of the $E(a)$ dependence and shifts the energy minimum slightly to larger values of *a*. The minima are found at 5.72 Å and 5.75 Å for U_{10} and U_{15}, respectively. These values correspond to a $\Delta a/a_{expt}$ of approximately +1.6% and are thus slightly higher than the experimental value. The effect of U_{eff} is that the total energies at the experimental lattice parameter are approximately 3 eV lower for U_{15} than for U_{10}. At the same lattice parameter, the total energy from the LSDA calculation is about6 eV higher than it is for U_{10}. It should be noted that the total energy given by the LDA+*U* calculation no longer corresponds to the LDA ground-state energy and thus may lead to erroneous conclusions about the structure. However, $E(a, U_{eff})$ will still give an indication of the optimal structure.

1. Magnetic moment and minority gap in the LDA+U

In the following, the dependence of the magnetic moments on the type of exchange-correlation functional is examined and compared with experimental values. The results of the calculations for Co_2FeSi, using different approximations for the potential as well as the parametrization of the exchange-correlation, are summarized in Table I.

Table I gives the site-resolved moments at Co and Fe sites and the total magnetic moment. The induced moment at the

TABLE I. Magnetic moments of Co_2FeSi. Values calculated for $a=5.64$ Å using different calculation schemes are given (see text). All values are given in μ_B. Total moments (m_{tot}) are given per unit cell, and site-resolved values (spin moment m_s, orbital moment m_l) are per atom. U was set to 15% of the atomic values. +SO indicates calculations that include the spin-orbit interaction.

	Co		Fe		Co_2FeSi
	m_s	m_l	m_s	m_l	m_{tot}
LSDA (vBH)	1.31		2.72		5.29
LSDA (VWN)	1.40		2.87		5.59
GGA (PBE)	1.39		2.85		5.56
GGA+SO	1.38	0.04	2.83	0.06	5.56
LDA+U	1.53		3.25		6.0
LDA+U+SO	1.56	0.08	3.24	0.07	6.0

Si sites (not given in Table I) was in all cases aligned antiparallel to that at the transition-metal sites. Likewise, the magnetic moment located in the interstitial is omitted in Table I; however, both quantities must be included to find the correct total moment.

The lowest value for the total magnetic moment was found using the von Barth–Hedin[32] (vBH) parametrization, and it differed from experiment by $-0.7\mu_B$. The results from the Vosko-Wilk-Nussair[44] parametrization and the GGA (Ref. 33) are very similar but still too low compared to the experimental value. It is seen that both site-specific moments are too low to reach the experimental value, which may need values of approximately $1.5\mu_B$ and $3\mu_B$ per atom at Co and Fe sites, respectively. This indicates that the LSDA or GGA approaches are not sufficient for explaining the magnetic structure of Co_2FeSi, independent of the type of parametrization that is used.

The correct magnetic moment at the experimental value of the lattice parameter was only found if the +U functional was used. Using the LDA+U scheme improves the total magnetic moment considerably (U_{15} was used for the calculations in Table I). The ratio of the magnetic moments of Co and Fe was measured to be $m_{Fe}/m_{Co}=2.2$ at 300 K in an induction field of 0.4 T.[12] The ratio of 2.1 found from the LDA+U calculations agrees very well with this value. The spin-orbit (SO) interaction was also included in some of the calculations to examine its influence on the total and partial magnetic moments. Including the SO interaction in the GGA calculations did not improve the total moment. The experiments delivered orbital to spin magnetic moment ratios (m_l/m_s) of approximately 0.05 for Fe and 0.1 for Co. The LDA+U+SO calculations produced values of 0.02 for Fe and 0.05 for Co, values that were factors of 2 smaller than the experimental values. Overall, the agreement of both ratios (m_{Fe}/m_{Co} and m_l/m_s) with experiment is better for the LDA+U than the pure LSDA or the GGA parametrization of the exchange-correlation functional. This may indicate that U corrects, at least partially, the missing orbital dependence of the potential in the LSDA.

In the following, the effect of the magnitude of the Coulomb exchange interaction on the magnetic moments will be discussed. Figure 6 compares the dependence of the magnetic moment on U_{eff} for Co_2FeSi and Co_2MnSi.

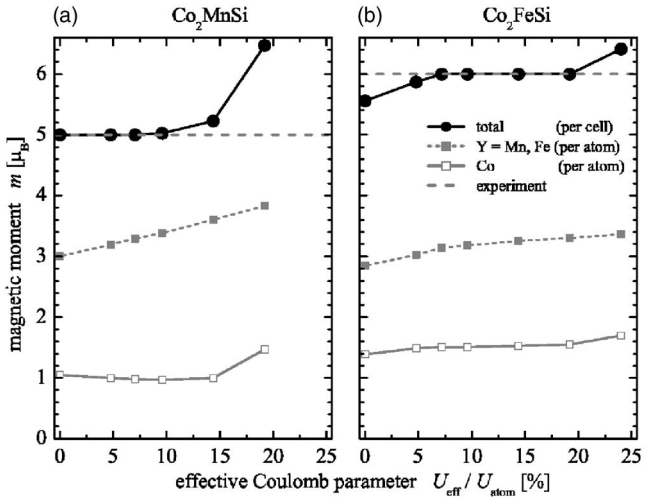

FIG. 6. Dependence of the magnetic moments on U_{eff}. The dashed horizontal lines indicate the experimental values of the magnetic moments for Co_2MnSi (a) and Co_2FeSi (b). The calculated values are connected by solid lines for clarity.

For Co_2FeSi, it is found that the total magnetic moment increases from $5.6\mu_B$ to $6\mu_B$ as U_{eff} increases from 0 to $U_{7.5}$ and stays at the integer value up to U_{20}. Above that value, the moment exhibits a further increase. The situation is different for Co_2MnSi, which has a total magnetic moment of $5\mu_B$ at a $U_{eff}=0$. The moment remains an integer up to approximately $U_{7.5}$ and then increases with increasing U_{eff}.

In Co_2MnSi, the moment at the Mn sites increases almost linearly with U_{eff}. At the same time, the moment decreases at the Co sites up to U_{10}, counterbalancing the Mn moments. At higher U_{eff}, the Co moment increases and the HMF character is lost. The situation is different in Co_2FeSi where both site-specific moments show an overall slight increase with increasing U_{eff}. Moreover, they stay rather constant in the range of $U_{7.5}-U_{20}$ so that the total moment remains an integer in this region. Being above the region of integer total moments in both materials, the moment at the Co sites reacts more strongly to U_{eff} than the moments at Y sites react to U_{eff}. The increase in the site-specific moments is much less pronounced in Co_2FeSi than in Co_2MnSi. This indicates that the Fe compound is much more stable against correlation effects than the Mn compound, at least as far as the magnetic moments are concerned.

It is again interesting to examine if the integer magnetic moment of Co_2FeSi is related to a real HMF gap in the minority band structure and to compare the behavior of the Co_2FeSi gap to the Co_2MnSi gap. The extremal energies of the gap enveloping bands are shown for both compounds in Fig. 7.

In both cases, the size of the gap increases with increasing U_{eff}. From Fig. 7(a), it is found that Co_2MnSi stays in an HMF state up to approximately U_8, which is the range of the integer magnetic moment. Larger values shift ϵ_F outside the gap. In Co_2FeSi [Fig. 7(b)], the minority gap includes ϵ_F from approximately U_8 to U_{20}. This means that the integer value of the magnetic moment is related to the minority gap in both compounds and is therefore a direct consequence of the HMF state.

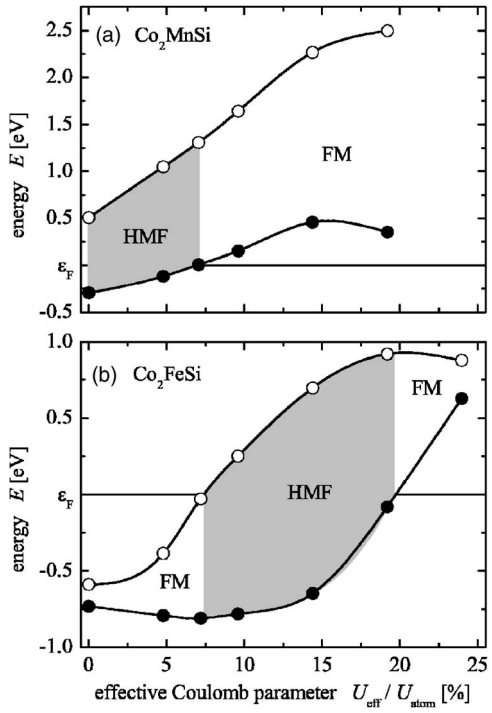

FIG. 7. Dependence of the minority gap on the effective Coulomb exchange parameter. The extremal energies of the gap involving states for Co_2MnSi (a) and Co_2FeSi (b) are shown. The shaded areas indicate the region of half-metallic ferromagnetism. Lines are drawn for clarity.

In both compounds, the gap is completely destroyed at very large values of U_{eff} ($\geqslant$8 eV). The effect of the Coulomb exchange interaction on single atoms (Co, Mn, or Fe) on the minority band gap was also investigated. As expected, it was found that the minority gap is destroyed in both materials if U_{eff} is added to only one of the 3*d* elements. However, small changes in only one of the U_{eff} values about the balanced value did not change the general behavior.

2. Electronic structure in the LDA+U

In the following, the influence of the correlation on the electronic structure will be discussed in more detail. Figure 8 compares the spin-resolved density of states for Co_2MnSi and Co_2FeSi that are calculated using the LSDA and LDA $+U$ approximations. The low-lying *sp* bands emerging from Γ_{5g} (majority) and Γ_{6g} (minority) *s* states are located at $(-8\cdots-10)$ eV. They are not shown here (compare with Fig. 4). These states are coupled to *p* states ($\Gamma_{5u,6u}$) and are mainly located at the Si atoms.

In both materials, the majority *d* states range from 8 eV below to approximately 4 eV above ϵ_F, where the onset of the high-lying, unoccupied *s* states becomes visible. *s* states are also present at below -4 eV due to the *s*-*d* coupling of the Γ_{5g} states. *p* states contribute to the density over the entire range of the *d* bands. When going away from the Γ point, they are mixed to *s* and *d* states because of the coupling of states with even and odd parity. The high density of states at -1 eV in Co_2MnSi or -2 eV in Co_2FeSi emerges mainly from Γ_{8g}-like states.

The situation is similar in the minority density of states where, in addition, a gap exists. This gap splits the minority *d* states and the unoccupied part above ϵ_F is mainly of Γ_{7g} character. As already has been discussed above, the minority gap is clearly different in both compounds and depends strongly on the applied effective Coulomb exchange interaction.

In the case of Co_2FeSi, where the experiment clearly indicates the total magnetic moment as having an integer value, the LSDA result seems to be incorrect. On the other hand, it should be noted that the unoccupied *d* states are sharply peaked at ϵ_F, resulting in a DOS that would imply an inherently unstable system in usual, simple ferromagnetic materials. This is despite the spin polarization. The system is, however, stabilized by the gap in the minority states that fixes the number of occupied states not only in the minority but also—and more importantly—in the majority channel. In the LDA, the paramagnetic e_g and t_{2g} states (located at the Co and Fe sites, respectively) are rather narrow at ϵ_F, suggesting that a Coulomb correlation of the Hubbard *U* type, which is ignored in the LSDA, will make Co_2FeSi insulating in the minority states. By attempting to treat electron correlation using the LDA$+U$ method, the electrons become more strongly localized. One of the major issues here is that the LDA$+U$ type correlation is important for the electronic and magnetic structure of Co_2FeSi. In more detail, the majority states at approximately -4 eV (arising from t_{2g} states in the paramagnetic case) are shifted by U_{15} to -6 eV below ϵ_F. At the same time, the unoccupied minority states, seen in the LSDA calculation just above ϵ_F, exhibit a larger shift of the paramagnetic e_g states (to 2 eV above ϵ_F) compared to the paramagnetic t_{2g} states (to 0.5 eV above ϵ_F). The occupied states of the minority DOS exhibit a less complicated behavior; they are mainly shifted towards the Fermi energy.

As shown in Fig. 8(b) for Co_2FeSi, U_{15} was chosen because the Fermi energy lies just in the middle of the gap for this value. It is clearly seen that the splitting between the occupied Γ_{8g} and unoccupied Γ_{7g} states becomes larger. The minority Γ_{7g} states exhibit an additional splitting after applying $+U$, whereas the unoccupied majority states stay rather unaffected. At the same time, the gap in the minority states becomes considerably larger and the Fermi energy is clearly within this gap, confirming that the compound is in an HMF state.

In Fig. 8(a), the DOS of Co_2MnSi is compared in the LSDA and LDA$+U$ approximations using U_{10}, which is above the limit for the HMF state. Being mainly located at the Co and Mn sites, the majority *d* states are clearly seen below ϵ_F and possess a width of approximately 7 eV. A low density of majority states emerging from strongly dispersing *d* bands is mainly found near ϵ_F. In the LSDA, there are hardly any minority states at ϵ_F, confirming that the compound is a half-metallic ferromagnet. Using the LDA$+U$, the *d* densities are found to be shifting away from ϵ_F, which is similar to what happens in Co_2FeSi. However, the occupied part of the minority DOS also changes if U_{eff} is applied: it shifts closer to the Fermi energy and crosses it for high values of U_{eff}. Once it reaches ϵ_F, the maximum value of U_{eff} that still results in the HMF state is attained, which is approximately $U_{7.5}$ in this case.

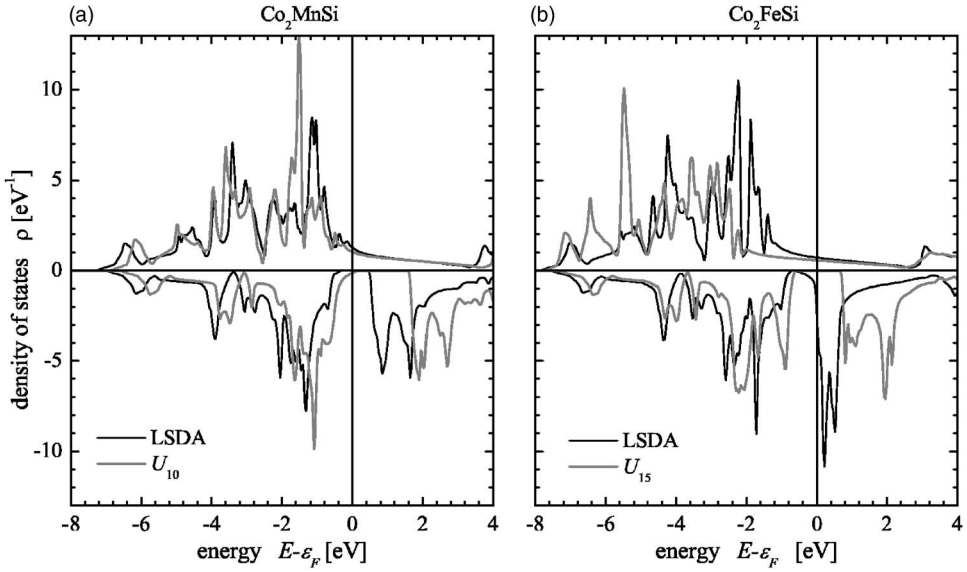

FIG. 8. Spin-resolved densities of states for Co_2MnSi and Co_2FeSi. Gray lines indicate the DOS using the LDA+U with U_{10} for Co_2MnSi (a) and U_{15} for Co_2FeSi (b). Black lines indicate the results from the LSDA. The upper and lower parts of the plots display the majority and minority states, respectively. (See text for the particular values of U at the different sites.)

Figure 9 shows the changes in the band structure of Co_2FeSi when the LDA+U method is applied. For easier comparison, details of the band structures are shown along Γ-X, which is the Δ direction of the paramagnetic state. The Δ direction is perpendicular to the Co_2 (100) planes. As was shown earlier[45] and as was also pointed out by Ögüt and Rabe,[46] just the Δ direction plays an important role in understanding the HMF character and magnetic properties of Heusler compounds.

The development of the band structure with increasing U_{eff} is shown in Fig. 9 for values of 1.26 eV, 2.52 eV, and 3.78 eV at the Co sites and, simultaneously, for values of 1.2 eV, 2.38 eV, and 3.56 eV at the Fe sites (U_5, U_{10}, and U_{15}). The upper panels (a)–(d) display majority band structures, and the lower panels (e)–(h) display the minority band structures. It is seen that only slight changes appear in the majority band structure, that the width of the visible bands at Γ stays rather unaffected, and that the main changes appear close to X.

More interesting is the behavior of the minority bands as these determine the HMF character of the compound. It is found that the energies of the occupied states at Γ stay nearly the same. The shapes of the bands close to Γ are similar as well. The situation is different at X, where the unoccupied states are shifted away from ϵ_F, resulting in a gap that increases with U_{eff}. It is clearly seen that this is an indirect gap. At U_{10}, the Fermi energy falls within the gap and the HMF state is reached. The minority gap is larger at Γ or at other points of high symmetry (not shown here) than at X. Therefore, it is obvious that the states at X determine the HMF character of the compound.

At this stage, it is clear that the gap in the minority states stays only within a certain range of the effective Coulomb exchange interaction. Outside of that limit, the Fermi energy

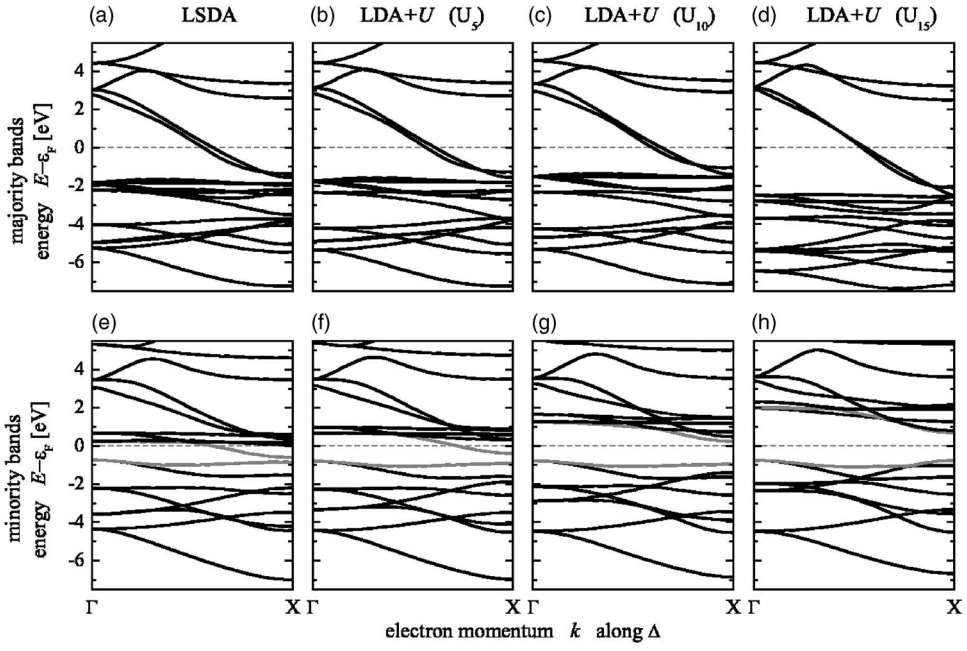

FIG. 9. Band structure of Co_2FeSi with variation of the Coulomb exchange interaction. The gray lines indicate the upper and lower bands defining the gap at the X point in the minority states. (See text for the particular values of $U_{\%}$ at the different sites.)

no longer falls inside the gap and the material loses its HMF character. It is also obvious that the same mechanism that leads to the half-metallic ferromagnetism in Co_2FeSi serves to destroy it in Co_2MnSi. The worst case for both materials would appear to be at approximately 7%–8% of the atomic values of U_{eff}, which is where the LDA+U still predicts values very close to the measured magnetic moments but which is also the borderline for the loss of the HMF character. This indicates that nearly integer magnetic moments alone do not verify the half-metallic ferromagnetism and that it may be necessary to search for alternative materials.

Previous band-structure calculations using the LSDA predicted Co_2MnSi to be an HMF at the experimental lattice parameter.[24,47] In the work presented here, LDA+U calculations were performed to examine the influence of on-site electron correlation in this compound. It was found that the gap in the minority DOS stays up to a U_{eff}=2.3 eV for Mn and a U_{eff}=2.5 eV for Co. For larger values of U_{eff}, which means stronger correlation, the system loses its HMF character because ϵ_F is shifted outside the minority gap. Co_2MnSi is expected to exhibit 100% spin polarization at the Fermi energy. This was not verified until now. Wang *et al.*[8] found only about 10% spin polarization at room temperature from a spin-resolved photoemission experiment. The spectra shown in Ref. 8 give no indication of the existence of a surface state that may serve to lower the spin polarization at ϵ_F. In the present work, it was found that even a moderate correlation will destroy the gap. If U_{10} is applied, then the spin polarization at ϵ_F is 75%, a value that is compatible to the approximately 55% found in Ref. 37. This indicates that on-site correlation might be one more reason why no complete spin polarization was found in this compound (for others, see Ref. 48).

Many effects have been considered in attempting to explain the missing experimental proof for complete spin polarization in predicted half-metallic ferromagnets.[48] Each of these effects may of course serve to reduce the spin polarization at the Fermi energy. On the other hand, none of these effects is able to explain a difference of 15% between the observed and calculated magnetic moments, as is the case for Co_2FeSi. The appearance of surface or interface states[49,50] may decrease the spin polarization in certain layers but will not drastically influence the measurements of the magnetization of bulk samples. Magnon excitations[51–55] will lead to a decrease of the magnetic moment with temperature rather than an increase and thus can be disregarded here. The spin-orbit interaction does indeed couple spin-up and spin-down states,[56] but as was shown above, does not enhance the magnetic moment. This may indicate that correlation might be one of the main causes for the too low spin polarization that is observed in experiments. In the presented work, a static correction was used in the LDA+U approximation. Dynamic correlation effects may be included in the LDA+DMFT approximation by using dynamical mean field theory (DMFT). Using this method for NiMnSb, it was shown by Chioncel *et al.*[57] that nonquasiparticle effects may also serve to change the properties of the gap in the minority states. The use of bulk-sensitive angle-, energy-, and spin-resolved photoemission becomes highly desirable for explaining the details of the band structure in the most complete experimental manner, as well as for proving the existence of correlation in predicted half-metallic ferromagnets and the actual existence of half-metallic ferromagnetism.

IV. SUMMARY AND CONCLUSIONS

Structural parameters, magnetic moments, and electronic properties of the Heusler compounds Co_2MnSi and Co_2FeSi were presented. Using LSDA or GGA calculations, the optimized lattice parameter that is obtained for Co_2FeSi results in a magnetic moment that is too small. The measured value of the magnetic moment was only found for a lattice parameter that was approximately 10% greater than the experimental value. In the LSDA or GGA approaches, it was also shown that the magnetic moment of Co_2MnSi is more stable against structural changes. At this time, it appears that simple LSDA and GGA methods are not sufficient for explaining the electronic structure of Heusler compounds in detail. At least for Co_2FeSi, these methods fail.

In a step beyond the basic LSDA and for the case of Co_2FeSi, it was shown that electron correlation is able to explain the experimental magnetic moment at the experimentally observed lattice parameter. It was found that the LDA+U scheme satisfactorily reproduces the experimental observations. At moderate effective Coulomb exchange-correlation energies of approximately 2.5–4.5 eV, the LDA+U calculations agreed very well with the measured total and site-specific magnetic moments. At the same time, the compound was clearly predicted to be a half-metallic ferromagnet.

How the inclusion of correlation would change the calculated properties of similar Heusler compounds was also examined. Co_2MnSi is a compound that is close to Co_2FeSi in the series of known Heusler compounds based on Co_2. It is obvious that on-site correlation will also play an important role in the Mn compound if it plays an important role in the Fe compound. It was found that a small correlation energy of only approximately 2.5 eV destroys the half-metallic ferromagnetism, which may explain why a complete spin polarization was not observed in this compound until now.

In conclusion, it is suggested that the inclusion of electron-electron correlation beyond the LSDA and GGA will be necessary to obtain a theoretical description of all potential half-metallic ferromagnets and for Heusler compounds in particular.

ACKNOWLEDGMENT

This work is financially supported by the DFG (research Project No. FG 559).

*Electronic address: felser@uni-mainz.de

[1] R. A. de Groot, F. M. Mueller, P. G. van Engen, and K. H. J. Buschow, Phys. Rev. Lett. **50**, 2024 (1983).
[2] S. Ishida, S. Fujii, S. Kashiwagi, and S. Asano, J. Phys. Soc. Jpn. **64**, 2152 (1995).
[3] P. J. Brown, K. U. Neumann, P. J. Webster, and K. R. A. Ziebeck, J. Phys.: Condens. Matter **12**, 1827 (2000).
[4] M. P. Raphael, B. Ravel, M. A. Willard, S. F. Cheng, B. N. Das, R. M. Stroud, K. M. Bussmann, J. H. Claassen, and V. G. Harris, Appl. Phys. Lett. **79**, 4396 (2001).
[5] U. Geiersbach, A. Bergmann, and K. Westerholt, J. Magn. Magn. Mater. **240**, 546 (2002).
[6] U. Geiersbach, A. Bergmann, and K. Westerholt, Thin Solid Films **425**, 225 (2003).
[7] S. Kämmerer, S. Heitmann, D. Meyners, D. Sudfeld, A. Thomas, A. Hütten, and G. Reiss, J. Appl. Phys. **93**, 7945 (2003).
[8] W. H. Wang, M. Przybylski, W. Kuch, L. I. Chelaru, J. Wang, Y. F. Lu, J. Barthel, and J. Kirschner, J. Magn. Magn. Mater. **286**, 336 (2005).
[9] W. H. Wang, M. Przybylski, W. Kuch, L. I. Chelaru, J. Wang, Y. F. Lu, J. Barthel, H. L. Meyerheim, and J. Kirschner, Phys. Rev. B **71**, 144416 (2005).
[10] K. Inomata, S. Okamura, and N. Tezuka, J. Magn. Magn. Mater. **282**, 269 (2004).
[11] S. Kämmerer, A. Thomas, A. Hütten, and G. Reiss, Appl. Phys. Lett. **85**, 79 (2004).
[12] S. Wurmehl, G. H. Fecher, H. C. Kandpal, V. Ksenofontov, C. Felser, H. J. Lin, and J. Morais, Phys. Rev. B **72**, 184434 (2005).
[13] S. Fuji, S. Sugimura, S. Ishida, and S. Asano, J. Phys.: Condens. Matter **2**, 8583 (1990).
[14] S. Ishida, T. Masakai, S. Fujii, and S. Asano, Physica B **245**, 1 (1998).
[15] M. P. Raphael, B. Ravel, Q. Huang, M. A. Willard, S. F. Cheng, B. N. Das, R. M. Stroud, K. M. Bussmann, J. H. Claassen, and V. G. Harris, Phys. Rev. B **66**, 104429 (2002).
[16] M. V. Yablonskikh, Y. M. Yarmoshenko, E. G. Gerasimov, V. S. Gaviko, M. A. Korotin, E. J. Kurmaev, S. Bartkowski, and M. Neumann, J. Magn. Magn. Mater. **256**, 396 (2003).
[17] A. Hütten, S. Kämmerer, J. Schmalhorst, and A. Thomas, Phys. Status Solidi A **201**, 3271 (2004).
[18] S. Picozzi, A. Continenza, and A. J. Freeman, Phys. Rev. B **69**, 094423 (2004).
[19] S. Picozzi, A. Continenza, and A. J. Freeman, J. Magn. Magn. Mater. **272-276**, 315 (2004).
[20] T. Block, M. J. Carey, B. A. Gurney, and O. Jepsen, Phys. Rev. B **70**, 205114 (2004).
[21] X. Y. Dong, C. Adelmann, J. Q. Xie, C. J. Palmstrom, X. Lou, J. Strand, P. A. Crowell, J.-P. Barnes, and A. K. Petford-Long, Appl. Phys. Lett. **86**, 102107 (2005).
[22] S. J. Hashemifar, P. Kratzer, and M. Scheffler, Phys. Rev. Lett. **94**, 096402 (2005).
[23] G. H. Fecher, H. C. Kandpal, S. Wurmehl, C. Felser, and G. Schönhense, J. Appl. Phys. (to be published).
[24] I. Galanakis, P. H. Dederichs, and N. Papanikolaou, Phys. Rev. B **66**, 174429 (2002).
[25] J. C. Slater, Phys. Rev. **49**, 931 (1936).
[26] L. Pauling, Phys. Rev. **54**, 899 (1938).
[27] J. Kübler, Physica B & C **127**, 257 (1984).
[28] P. J. Webster and K. R. A. Ziebeck, in *Alloys and Compounds of d-Elements with Main Group Elements.* edited by H. P. J. Wijn, Landolt-Börnstein, New Series, Group III, Vol. 196, pt. 2 (Springer-Verlag, Heidelberg, 1988), pp. 104–185.
[29] P. J. Webster and K. R. A. Ziebeck, J. Phys. Chem. Solids **34**, 1647 (1973).
[30] F. Heusler, Verh. Dtsch. Phys. Ges. **12**, 219 (1903).
[31] P. Blaha, K. Schwarz, G. K. H. Madsen, D. Kvasnicka, and J. Luitz, Computer code WIEN2k, an augmented plane wave +local orbitals program for calculating crystal properties, Karlheinz Schwarz, Techn. Universitaet Wien, Wien, Austria, 2001.
[32] U. v. Barth and L. Hedin, J. Phys. C **5**, 1629 (1972).
[33] J. P. Perdew, K. Burke, and M. Ernzerhof, Phys. Rev. Lett. **77**, 3865 (1996).
[34] V. I. Anisimov, F. Aryasetiawan, and A. I. Lichtenstein, J. Phys.: Condens. Matter **9**, 767 (1997).
[35] V. Niculescu, T. J. Burch, K. Rai, and J. I. Budnick, J. Magn. Magn. Mater. **5**, 60 (1977).
[36] L. Ritchie, G. Xiao, Y. Ji, T. Y. Chen, C. L. Chien, M. Zhang, J. Chen, Z. Liu, G. Wu, and X. X. Zhang, Phys. Rev. B **68**, 104430 (2003).
[37] L. J. Singh, Z. H. Barber, Y. Miyoshi, Y. Bugoslavsky, W. R. Branford, and L. F. Cohen, Appl. Phys. Lett. **84**, 2367 (2004).
[38] J. J. Kübler, A. R. Williams, and C. B. Sommers, Phys. Rev. B **28**, 1745 (1983).
[39] J. H. van Vleck, Rev. Mod. Phys. **25**, 220 (1953).
[40] J. C. Slater, Phys. Rev. **49**, 537 (1936).
[41] P. Fulde, *Electron Correlations in Molecules and Solids*, 3rd ed. (Springer-Verlag, Heidelberg, 1995).
[42] I. V. Solovyev and M. Imada, Phys. Rev. B **71**, 045103 (2005).
[43] R. D. Cowan, *The Theory of Atomic Structure and Spectra* (University of California Press, Berkeley, 1981).
[44] S. H. Vosko, L. Wilk, and M. Nussair, Can. J. Phys. **58**, 1200 (1980).
[45] G. H. Fecher, H. C. Kandpal, S. Wurmehl, J. Morais, H.-J. Lin, H.-J. Elemrs, G. Schönhense, and C. Felser, J. Phys.: Condens. Matter **17**, 7237 (2005).
[46] S. Ögüt and K. M. Rabe, Phys. Rev. B **51**, 10443 (1995).
[47] S. Picozzi, A. Continenza, and A. J. Freeman, Phys. Rev. B **66**, 094421 (2002).
[48] P. A. Dowben and R. Skomski, J. Appl. Phys. **95**, 7453 (2004).
[49] G. A. de Wijs and R. A. de Groot, Phys. Rev. B **64**, 020402 (2001).
[50] S. J. Jenkins and D. A. King, Surf. Sci. Lett. **501**, L185 (2002).
[51] M. H. Jo, N. D. Mathur, N. K. Todd, and M. G. Blamire, Phys. Rev. B **61**, R14905 (2000).
[52] J. M. D. Coey and M. Venkatesan, J. Appl. Phys. **91**, 8345 (2002).
[53] C. N. Borca, T. Komesu, H.-K. Jeong, P. A. Dowben, D. Ristoiu, C. Hordequin, J. P. Nozieres, J. Pierre, S. Stadler, and Y. U. Idzerda, Phys. Rev. B **64**, 052409 (2001).
[54] C. Hordequin, J. Pierre, and R. Currat, Physica B **234-236**, 605 (1997).
[55] C. Hordequin, D. Ristoiu, L. Rannoa, and J. Pierre, Eur. Phys. J. B **16**, 287 (2000).

[56] P. Mavropoulos, K. Sato, R. Zeller, P. H. Dederichs, V. Popescu, and H. Ebert, Phys. Rev. B **69**, 054424 (2004).

[57] L. Chioncel, M. I. Katsnelson, R. A. de Groot, and A. I. Lichtenstein, Phys. Rev. B **68**, 144425 (2003).

[58] This is true for ternary Heusler compounds, but may be different in quaternary compounds with noninteger site occupancies.

[59] This also affects the exchange integrals for *f* electrons; compare Ref. 43 Table 6-1, p. 165 and Ref. 34.